ACS APPLIED MATERIALS & INTERFACES

RESEARCH ARTICLE

www.acsami.org

# Synergistic Catalytic Effect of a Composite (CoS/PEDOT:PSS) Counter Electrode on Triiodide Reduction in Dye-Sensitized Solar Cells

P. Sudhagar,[†] S. Nagarajan,[†] Yong-Gun Lee,[‡] Donghoon Song,[†] Taewook Son,[†] Woohyung Cho,[†] Miyoung Heo,[†] Kyoungjun Lee,[†] Jongok Won,[§] and Yong Soo Kang[†,*]

[†]Center for Next Generation Dye-Sensitized Solar Cells, WCU Program Department of Energy Engineering, Hanyang University, Seoul 133-791, South Korea.

[‡]School of Chemical and Biological Engineering, Seoul National University, Seoul, South Korea

[§]Department of Chemistry, Sejong University, Seoul, South Korea

Supporting Information

**ABSTRACT:** Inorganic/organic nanocomposite counter electrodes comprised of sheetlike CoS nanoparticles dispersed in polystyrenesulfonate-doped poly(3,4-ethylenedioxythiophene (CoS/PEDOT:PSS) offer a synergistic effect on catalytic performance toward the reduction of triiodide for dye-sensitized solar cells (DSSCs), yielding 5.4% power conversion efficiency, which is comparable to that of the conventional platinum counter electrode (6.1%). The electrochemical impedance spectroscopy (EIS) and cyclic voltammetry measurements revealed that the composite counter electrodes exhibited better catalytic activity, fostering rate of triiodide reduction, than that of pristine PEDOT: PSS electrode. The simple preparation of composite (CoS/PEDOT:PSS) electrode at low temperature with improved electrocatalytic properties are feasible to apply in flexible substrates, which is at most urgency for developing novel counter electrodes for lightweight flexible solar cells.

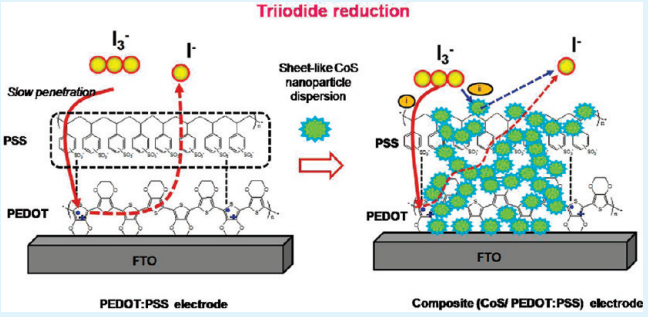


**KEYWORDS:** counter electrode, CoS, PEDOT:PSS, dye-sensitized solar cells, impedance spectroscopy

## 1. INTRODUCTION

Dye-sensitized solar cells (DSSCs) offer promising performance (~11%) at low costs compared to conventional p−n junction silicon solar cells and, therefore, have been lauded as next-generation solar cells.[1,2] The exploration of alternative counter electrodes to replace expensive, corrosive platinum (Pt) in dye-sensitized solar cells (DSSCs) is one of the future avenues for improving DSSC performance and stability at a low cost. Considerable research has been dedicated to the development of Pt-free counter electrodes using carbon and conducting polymer electrodes.[3−9] Recently, polystyrenesulfonate-doped poly(3,4-ethylenedioxythiophene) (PEDOT:PSS) electrodes demonstrated feasible performance among Pt-free counter electrodes due to their unique characteristics, such as rather high conductivity (up to 550 S/cm when highly doped), electrocatalytic activity, good film-forming ability, and relatively low cost.[10] However, these electrodes exhibit a poor fill factor (~30−50%) because of the large size of the dopant PSS chains, which may be directly exposed to $I_3^-/I^-$, preventing the contacts or interactions between the active sites of PEDOT chains and $I_3^-/I^-$.[11−13] The poor performance has also been attributed to the difficulty $I_3^-$ experiences in penetrating PEDOT chains, resulting in a low fill factor.[11]

These limitations were improved upon in two ways, substituting dopants and incorporating inorganic nanomaterials in PEDOT:PSS. For instance, low-molecular-weight sodium p-toluene sulfonate (TsO) was introduced instead of PSS to hamper the direct contact between PSS chains and $I_3^-/I^-$.[14] Carbon-based composite materials such as carbon nanotubes (CNTs)[15] and graphene[16] incorporated into PEDOT:PSS resulted in higher catalytic performance than pristine PEDOT:PSS. Although a variety of semiconductor electrocatalytic materials are available in addition to carbon-based composite materials, efforts are still needed to find suitable materials that may enhance the catalytic performance of PEDOT:PSS. Increasing the triiodide reduction reaction at the counter electrode may result in the improvement of the energy conversion efficiency. It is anticipated that inclusion of nanostructured scaffold may provide the higher catalytic activity and the enlarged surface area for the reduction reaction at the counter electrode side. In addition, it can be easily synthesized in low cost and capable to show comparable catalytic effects with Pt electrode.

In the present work, we report the synergistic catalytic effect of a nanocomposite counter electrode comprised of cobalt sulfide (CoS) nanomaterials incorporated into PEDOT:PSS as shown

Received: November 18, 2010
Accepted: May 13, 2011
Published: May 13, 2011

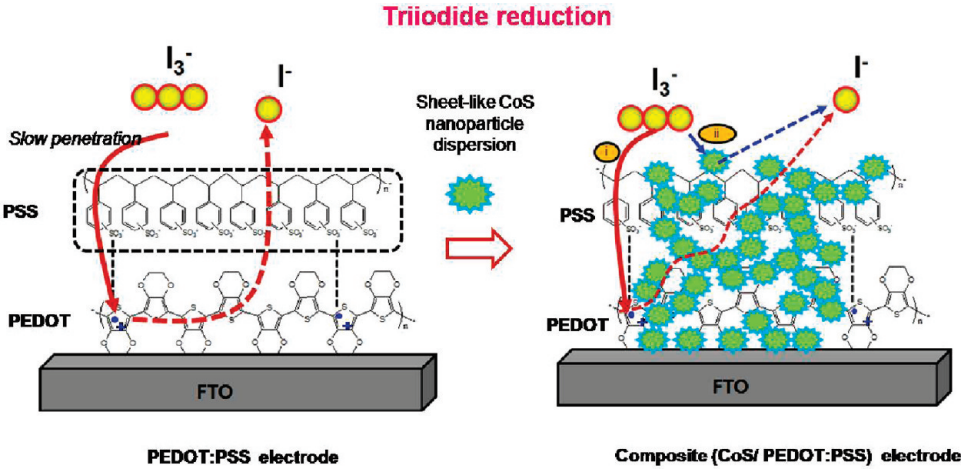


**Figure 1.** Schematic of triiodide reduction at (a) pristine PEDOT:PSS and (b) composite sheetlike CoS nanoparticles dispersed in PEDOT:PSS electrode (note that the $I_3^-$ was reduced to $I^-$ through both (i) PEDOT:PSS and (ii) CoS).

in Figure 1. CoS has additional advantages for large-scale applications as it is much more abundant and cheaper than Pt. It was recently reported that quasi-transparent CoS counter electrode (coated on ITO/PEN) showed comparable electrocatalytic performance with conventional Pt for the reduction of triiodide. The long-term stability was tested by subjecting it to light soaking at 60 °C for 1000 h and the energy conversion efficiency retained 85% of its initial value.[17] Therefore beneficial advantages of introducing composite material, sheetlike CoS, are (i) catalytic effects toward tri-iodide reduction and (ii) filler effects helping contacts between PEDOT and $I_3^-$ as schematically drawn in Figure 1b.

## 2. EXPERIMENTAL SECTION

**Materials.** Cobalt nitrate, thiourea, hexamethylenetetramine, iodine, and PEDOT:PSS (1.3 wt % dispersed in $H_2O$, conductive grade, product number: 483095) were purchased from Sigma Aldrich and used as received without further purification. $TiO_2$ paste (Ti-nanooxide T20/SP) and N719 dye ($Ru(dcbpy)_2(NCS)_2$(dcbpy = 2,2-bipyridyl-4, 4-dicarboxylato) were purchased from Solaronix, Switzerland. MPII (1-methyl-3-propylimidazolium iodide) was purchased from Merck, Germany.

**Synthesis of CoS Nanostructures.** A typical synthetic method of CoS nanostructures was as follows: 40 mL of 0.1 M cobalt nitrate solution in deionized water was added slowly to the 40 mL of 0.1 M thiourea solution in 40 mL of deionized water. The mixed solution was kept stirring for 30 min. For preparing sheetlike CoS nanostructures, we added a structure-directing agent 0.1 M hexamethylenetetramine (HTA) in water into the above solution. Finally, the resultant solution was transferred to a Teflon-lined autoclave and kept at 180 °C for 24 h. After the desired period of hydrothermal reaction was completed, the autoclave vessel was cooled to room temperature, and the product was obtained by centrifuging at 2000 rpm. The resultant product was washed with ethanol and deionized water repeatedly and dried at 80 °C for 3 h.

**Preparation of Counter Electrodes.** Pristine and nanocomposites electrodes comprising CoS dispersed in the PEDOT:PSS matrices were prepared on precleaned fluorine-doped tin oxide (FTO) substrates (Pilkington, USA, sheet resistance 12 Ω/sq) by spin coating technique. The pristine PEDOT:PSS counter electrode was fabricated using PEDOT:PSS solution at 2000 rpm for 60 s. In the case of composite electrodes, 0.1 wt % of the as-synthesized CoS were dispersed in 1 wt % PEDOT:PSS solution in deionized water, and sonicated for 15 min. Further, it kept under stirring for 12 h for making well dispersed composite solutions. The composite electrodes were abbreviated as CoS/PEDOT:PSS. All the films prepared from spin coating were further sintered at 120 °C for 2 h at ambient atmosphere. For preparing CoS counter electrodes, the as-synthesized CoS nanopowder was dispersed with alpha teriphenol/ethyl cellulose colloidal and spreaded on FTO substrates by spin-coating. Subsequently, electrodes were sintered at 350 °C for 30 min. In addition, a reference counter electrode (Pt) was prepared by spin-coating from 0.01 M $H_2PtCl_6$ solution in isopropanol and subsequently by sintering at 450 °C for 30 min at ambient atmosphere.

**Fabrication of DSSCs.** $TiO_2$ working photoanodes about ~12 $\mu$m were prepared on FTO substrate using $TiO_2$ paste by doctor blade technique and subsequently sintered at 450 °C for 30 min in ambient atmosphere. To avoid the back travel electron flow from FTO substrate to electrolyte, a thin $TiO_2$ blocking layer was prepared in between the $TiO_2$ photoanode and the FTO layer by spin coating of 2 wt % Ti (IV) bis(ethyl acetylacetonate) di-isopropoxide solution in 1-butanal and subsequent calcination at 450 °C for 30 min. N719 dye was used to sensitize the $TiO_2$ photo electrodes. $TiO_2$ electrodes were immersed overnight in the 0.3 mM dye solution containing a mixture of acetonitrile (ACN) and t-butyl alcohol (1:1 v/v) and dried at room temperature. A sandwich-type configuration was employed to measure the performance of the dye-sensitized solar cells, using a Pt-coated F-doped $SnO_2$ film as a counter electrode and 0.1 M LiI, 0.5 M MPII (1-methyl-3-propylimidazolium iodide), 0.5 M tBP, 0.05 M GuSCN, with 0.05 M $I_2$ in ACN as the electrolyte solution.

**Characterization.** Current−voltage characteristics of DSSCs were obtained under 1 sun illumination (AM 1.5G, 100 mW $cm^{-2}$) with a Newport (USA) solar simulator (300W Xe source) and a Keithley 2400 source meter (active area is 0.25 $cm^2$ with shadow mask). Electrochemical impedance measurements were carried out under light illumination (100 mW $cm^{-2}$) using a potentiostat (IM6, ZAHNER) equipped with a frequency response analyzer (Thales) in the frequency range of 0.1 Hz−1000 kHz. The results were analyzed with an equivalent circuit model for interpreting the characteristics of the DSSCs. Incident photon-to-current conversion efficiency (IPCE) of DSSCs was measured using Model QEX7 (PV Measurements Inc.) with reference to the calibrated silicon diode. The cyclic voltammogram (CV) was measured in a three-electrode electrochemical cell using a Zahner potentiostat with the pristine or the CoS/PEDOT:PSS working electrodes, Pt-foil counter electrode and Ag/AgCl reference electrode dipped in an acetonitrile solution of 10 mM LiI, 1 mM $I_2$ and 0.1 M $LiClO_4$. (scan

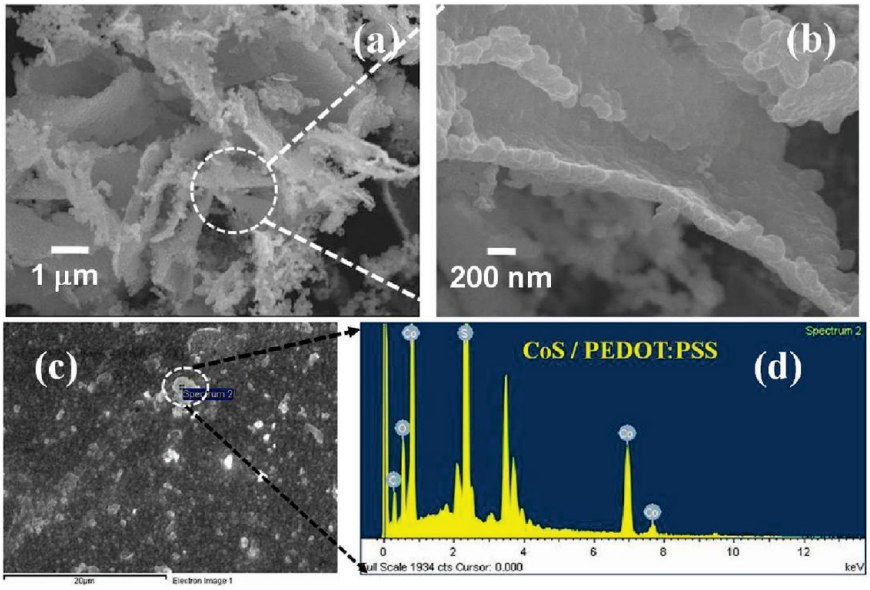


**Figure 2.** (a, b) SEM images of as-synthesized sheetlike CoS and (d) energy-dispersive spectrum of CoS/PEDOT:PSS composite film.

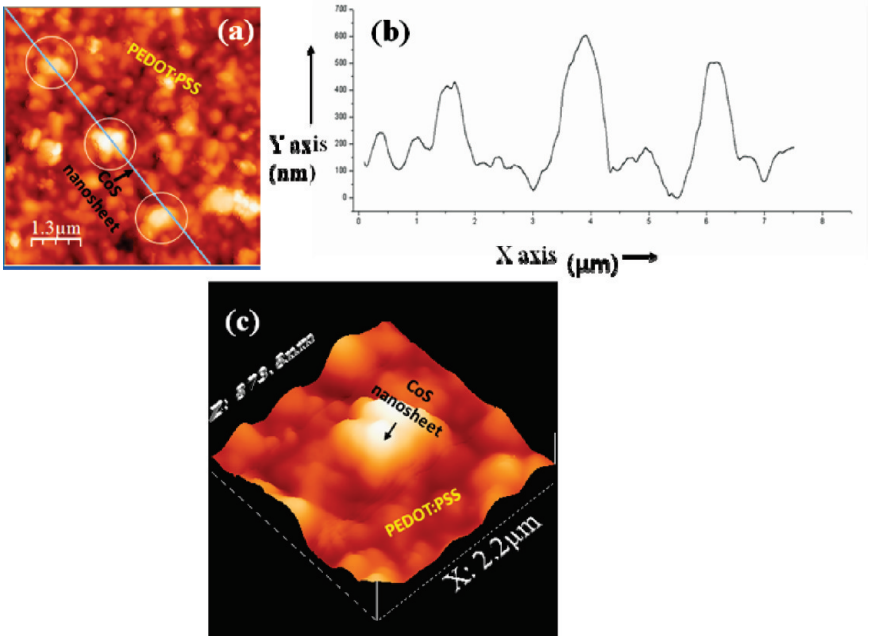


**Figure 3.** (a) AFM images of the sheetlike CoS dispersed in PEDOT:PSS and (b) surface profile of the sheetlike CoS on PEDOT:PSS matrix, and (c) CoS/PEDOT:PSS interface.

condition: 50 mV $s^{-1}$). The surface topography of the coated samples was investigated using atomic force microscopy (AFM), (Nanoscope, Dimension-3100 Multimode), and the AFM tip was a silicon-SPM sensor (tapping mode), thickness 4 $\mu$m, length 125 $\mu$m and width 30 $\mu$m. Surface morphology of the samples was studied using field-emission scanning electron microscope (FESEM) (JEOL-JSM6340).

## 3. RESULTS AND DISCUSSION

**Morphology.** The structural features of the CoS nanostructures produced from a hydrothermal reaction were studied by scanning electron microscopy (SEM), as shown in Figure 2. From images a and b in Figure 2, we found that sheetlike aggregate structures of CoS primary particles were formed. The primary particle size was approximately 200 nm. The constituents of the CoS nanostructures in PEDOT:PSS matrices were confirmed through energy-dispersive analysis (Figure 2d). Good interfacial adhesion resulted from spin-coating this composite solution into a thin film on a substrate. Additionally, we observed that the resulting composite film was mechanically stable and did not peel from the substrate in water during the electrolyte filling process. AFM images of the CoS/PEDOT:PSS film show that CoS composite particles were well-dispersed in the PEDOT:PSS matrix (Figure 3).

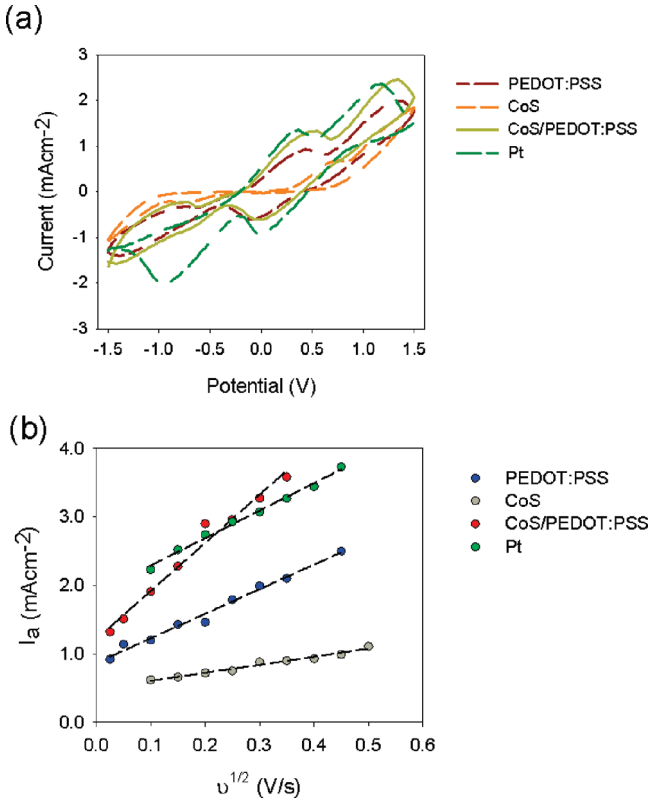


**Figure 4.** Cyclic voltammograms of pristine PEDOT:PSS, CoS, CoS/PEDOT:PSS, and Pt electrodes using symmetry cell configuration (electrolyte containing methoxypropionitrile solvent with 10 mM LiI, 1 mM $I_2$ and 0.1 M $LiClO_4$) measured scan rate of 50 $mVs^{-1}$.

**Electrochemical Analysis.** Cyclic voltammograms (CVs) of the $I_3^-/I^-$ system in the pristine PEDOT:PSS, CoS and CoS/PEDOT:PSS composite counter electrodes and the Pt electrode are presented in Figure 4. The Pt electrodes showed two peaks: the negative peak is associated with the reduction of tri-iodide ($I_3^- + 2e^- \rightarrow 3I^-$), and the positive peak is associated with the oxidation reaction ($3I_2^- + 2e^- \rightarrow 2I_3^-$).[18] The redox current density of $I_3^-/I^-$ in the pristine PEDOT:PSS electrode is smaller than that in the Pt electrode. In DSSCs, electrons generated from the oxidation of $I^-$ ions to form $I_3^-$ regenerate photooxidized dyes, and the produced $I_3^-$ ions diffuse to and are reduced at the counter electrode. It has been reported that the reduction reaction rate is very slow on the pristine PEDOT:PSS electrode,[11] which might affect the dye-regeneration at the photoanode.[19] The current density increased when CoS nanosheets were incorporated into the PEDOT:PSS electrodes, suggesting the enhanced electrocatalytic activity of the counter electrode in reducing $I_3^-$. One possible reason may be the improved catalytic activities of both the CoS nanoparticles by forming sheet-like structure and the PEDOT:PSS by the filler effects rendering better contacts between the PEDOT:PSS and $I_3^-$. much easily due to the CoS nanoparticles. Therefore, nanocomposite electrodes comprising 2D sheetlike CoS nanoparticle incorporated into a PEDOT:PSS matrix render a synergistic catalytic effect compared to either pristine PEDOT:PSS or CoS electrodes.

To gain better insight in the catalytic process of tri-iodide reduction, diffusivity of $I_3^-$ redox species at different counter electrodes (symmetric cell configuration) was investigated.

**Table 1. Photovoltaic Properties of DSSCs with Various Counter Electrodes under 100 mW $cm^{-2}$, AM 1.5G Illumination**

| counter electrode | $V_{oc}$ (V) | $J_{sc}$ ($mAcm^{-2}$) | FF (%) | efficiency (%) |
|---|---|---|---|---|
| PEDOT:PSS | 0.66 | 11.6 | 49.5 | 3.8 |
| CoS | 0.59 | 4.42 | 39.6 | 1.0 |
| CoS/PEDOT:PSS | 0.65 | 13.2 | 62.7 | 5.4 |
| Pt | 0.69 | 13.0 | 67.1 | 6.1 |

The anodic peak current ($I_p$) values of cyclic voltammogram (Figure 4a) were collected at different scan rates (see the Supporting Information). Figure 4b shows the linear relationship between anodic peak current and square root of the scan rate for all counter electrodes. This inferred that the reduction reaction of $I_3^-/I^-$ redox couples at counter electrodes was diffusion-controlled and obeyed the Randles-Sevcik equation. In fact, the diffusion coefficient is proportional to the $I_{lim}$ as per eq 1.[20]

$$I_p = KnFAC^*(nF/RT)\upsilon^{1/2}D_o^{1/2} \quad (1)$$

where $K$ is the constant ($2.69 \times 10^5$); $A$ is the interelectrode distance; n = 2, the number of electrons contributing the charge transfer; $F$ is Faraday's Constant; $C^*$ = bulk concentration of triiodide species. The diffusion coefficients of $I_3^-$ at different counter electrodes were estimated and listed in Table 2. It clearly shows that the diffusivity with the pristine PEDOT: PSS electrode ($D_n$ =5.12 $\times$ $10^{-6}$ $cm^{-2}$ $s^{-1}$) was apparently improved to $D_n$ =1.96 $\times$ $10^{-5}$ $cm^{-2}$ $s^{-1}$ by inclusion of CoS composite materials, which was even slightly larger than Pt electrode. This offer more options for bringing synergetic effects of CoS/PEDOT:PSS nanocomposite electrode in catalytic performance compared to pristine CoS or PEDOT:PSS electrode.

**Photovoltaic Performance.** Table 1 summarizes the photovoltaic parameters obtained from photocurrent−voltage ($J-V$) curves (Figure 5) of DSSCs with three different counter electrodes measured under the illumination of 1 sun (100 mW $cm^{-2}$). The Pt counter electrode showed a conversion efficiency of about 6.1%, and the CoS/PEDOT:PSS electrode achieved a conversion efficiency of 5.4%, a performance comparable to that of Pt. The pristine PEDOT:PSS, however, achieved a conversion efficiency of 3.8%, much lower than that of the CoS/PEDOT:PSS films, mainly due to a lower fill factor of 0.49.[11] Furthermore, the higher photocurrent density of the CoS/PEDOT:PSS electrode ($J_{sc}$ = 13.2 mA $cm^{-2}$) with respect to that of the pristine electrode may arise from the efficient reduction reaction in the $I_3^-/I^-$ system, as was discussed in the CV analysis (Figure 4). The overall characteristics of CoS/PEDOT:PSS composite counter electrodes reveal their reliable performance comparable with that of conventional Pt counter electrodes. The IPCE spectra are shown in the inset of Figure 5. The CoS/PEDOT:PSS counter electrode showed a higher external quantum efficiency than that of the pristine PEDOT:PSS electrode. The high external quantum efficiency can be explained by the efficient reduction of $I_3^-/I^-$ at the composite electrode, resulting in fast dye regeneration at the photoanode and high photocurrent.

To decipher the role of CoS in composite counter electrodes further, different amount of the CoS nanoparticles was blended with PEDOT:PSS matrix and their $J-V$ performance were studied (see the Supporting Information, SI2). The photoconversion efficiency of the composite system was gradually

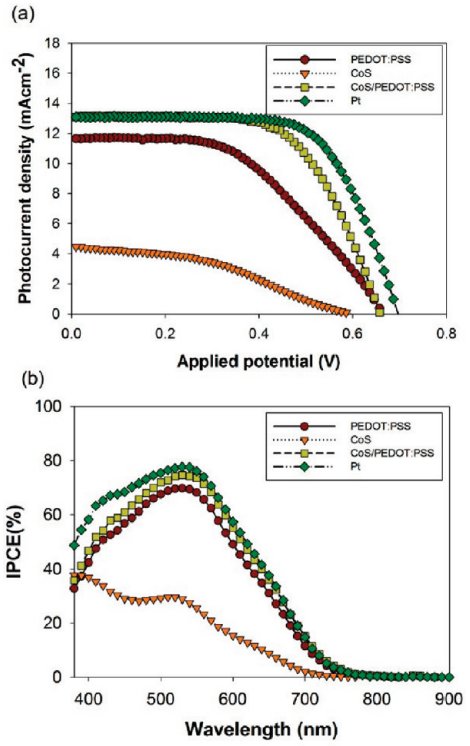


**Figure 5.** (a) Current−voltage characteristics of DSSCs based on pristine PEDOT:PSS, CoS/PEDOT:PSS and Pt counter electrodes under light illumination (100 mW $cm^{-2}$) and (b) IPCE spectra of DSSCs using different counter electrodes.

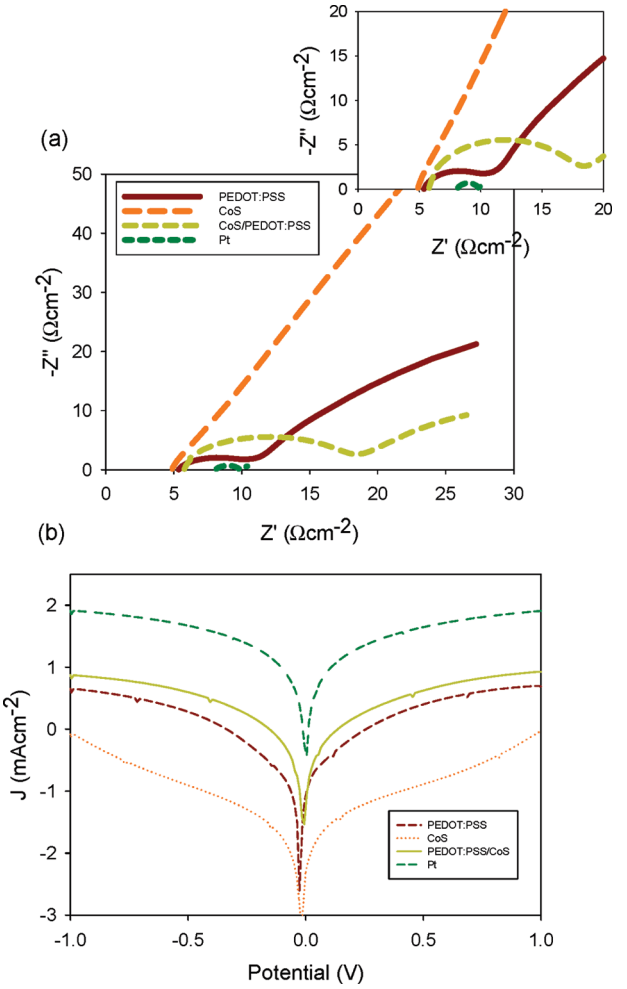


**Figure 6.** (a) Nyquist spectra of DSSCs using different counter electrodes; inset shows enlarged higher-frequency region for clarity. (b) Tafel plot.

improved with increasing CoS content up to 1 wt %. The linear increase in $J_{sc}$ and fill factor with the CoS content reflects the improvement of the catalytic activity of counter electrodes, which supports the improved dye regeneration rate by the efficient $I_3^-$ reduction. However, as the content of CoS was further increased to 2%, the energy conversion efficiency of the DSCs decreased to 0.4%, which was even lower than that of DSCs based on the pristine PEDOT:PSS electrode. Though sheetlike CoS particles play a crucial role in the catalytic reduction, more CoS may block the interfacial contacts between PEDOT chains and $I_3^-$. The blockage of PEDOT catalytic effect obliviously may reduce the regeneration rate of dye molecules and consequently the photocurrent density as low as 2.7 mAcm$^{-2}$. Therefore we conclude that 1 wt % of the sheetlike CoS is optimum for the PEDOT:PSS matrix for achieving better conversion efficiency. It should be noted that the energy conversion efficiency of the reference cell using Pt electrode is comparatively low (6.1%), compared to conventional cells. The low $J_{sc}$ and $V_{oc}$ may be mostly associated with many reasons irrespective of the counter electrode. Further, the cell performance will be improved by implementing (a) introduction of a scattering layer, (b) $TiCl_4$ treatment of photoanode, (c) introduction of a suitable coadsorbent, and/or (d) better electrolyte compositions including additives.

**Electrochemical Impedance Analysis.** To investigate the charge-transport phenomena at the TCO/counter electrode/electrolyte interface we performed, electrochemical impedance analysis using a thin symmetric cell; the resulting Nyquist spectra are given in Figure 6. The charge transfer resistance ($R_{ct}$) at the counter electrode was estimated from the diameters of the leftmost semicircles using ZSim software with the Randles circuit (see the Supporting Information, SI3).[21] The estimated $R_{ct}$ values of counter electrodes are listed Table 2. The charge transfer resistance of the neat PEDOT:PSS (2.65 Ω cm$^{-2}$) was apparently increased after inclusion of the CoS composite particles (6.15 Ω cm$^{-2}$). However, the Nernst diffusion resistance (estimated from the diameter of semicircle at low frequency) of the composite electrode (39 Ω cm$^{-2}$) was lesser than the pristine PEDOT:PSS electrode (85.5 Ω cm$^{-2}$), presumably arising from the improvement of the surface roughness of the electrode (see the Supporting Information, SI1). In addition beneficial effect of CoS filler effect on PEDOT:PSS molecular structure, which hindering the active role of $PSS^-$ chains also enhance the diffusivity $I_3^-$ redox carrier (mass transfer) to the counter electrode. This argument is in line with the estimated diffusion coefficient values from CV analysis (table 2).

Furthermore, a higher exchange current (log $I_0$) at the nanocomposite counter electrode compared to that at the pristine electrode was obtained, as calculated from the Tafel eq 2 and the cathodic and anodic polarization data (Figure 6b).[22]

$$I = nFAK_s\{C_o^{surf}\exp((\alpha nF)\eta/RT) - C_R^{surf}\exp((\beta nF)\eta/RT) \quad (2)$$

**Table 2. Electrochemical Impedance Parameters of DSSCs with Various Counter Electrodes**

| counter electrode | $R_{ct}$[aa] ($\Omega$ cm$^{-2}$) | $W_R$[aa] ($\Omega$ cm$^{-2}$) | og$I_0$[ba] (mA cm$^{-2}$) | $D_n$[ca] (cm$^{-2}$s$^{-1}$) |
|---|---|---|---|---|
| PEDOT:PSS | 2.65 | 85.5 | $8.99 \times 10^{-5}$ | $5.12 \times 10^{-6}$ |
| CoS | 5.91 | 917.4 | $1.03 \times 10^{-5}$ | $5.40 \times 10^{-7}$ |
| CoS/PEDOT:PSS | 6.15 | 39.0 | $2.54 \times 10^{-4}$ | $1.96 \times 10^{-5}$ |
| Pt | 0.35 | 2.4 | $4.35 \times 10^{-5}$ | $6.39 \times 10^{-6}$ |

[a] Values derived from a, impedance spectra; b, Tafel plot; and c, cyclicvoltammogram.

Where $I$ is the electrode current, $A$ is the electrode active surface area, $K_s$ is the standard equilibrium constant, $\eta$ is the over potential, $C_o^{surf}$ is the reactant concentration near the electrode, $C_R^{surf}$ is the product concentration near the electrode, and $\alpha$ and $\beta$ are anodic and cathodic transfer coefficients, respectively. The exchange current can be calculated from the intersection of the linear anodic and cathodic curves. This also demonstrates that the rough surface of the nanocomposite electrode remarkably enhances the electrochemical triiodide reduction reaction rate by superimposing the properties of CoS onto PEDOT:PSS, which undoubtedly accounts for the high photovoltaic performance. Tafel plot was used to study the interfacial charge-transfer properties of the $I_3^-/I^-$ redox couple in the symmetric cell configuration (electrode/electrolyte/electrode) using different counter electrodes. The experimental polarization curves were fitted with the Butler–Volmer eq 2, describing the dependence of electrical current on electrode potential, by assuming that both cathodic and anodic reactions occur on the same electrode.

## 4. CONCLUSIONS

CoS/PEDOT:PSS nanocomposite counter electrodes utilizing CoS nanosheets made of primary particles 200 nm in diameter resulted in much higher catalytic activity for the reduction reaction than either pristine CoS or PEDOT:PSS electrode. Consequently, a much higher conversion efficiency of 5.4% under 1 sun illumination was achieved. High exchange currents with 2-D sheet-like CoS nanostructures/PEDOT:PSS render desirable counter electrode properties in DSSCs. Furthermore, the simple preparation at low temperature and inexpensive cost of CoS nanosheets opens up new avenues for counter electrodes using flexible substrates, which may not be feasible with conventional Pt electrodes. We believe that the current work paves the way for the development of a new generation of highly efficient, low-cost DSSCs using composite counter electrodes.

## ■ ASSOCIATED CONTENT

**Supporting Information.** Schematic of thin layer symmetry cells and equivalent circuit of electrochemical impedance spectroscopy. This material is available free of charge via the Internet at http://pubs.acs.org.

## ■ AUTHOR INFORMATION

**Corresponding Author**
*E-mail: kangys@hanyang.ac.kr.

## ■ ACKNOWLEDGMENT

This work was supported by the Engineering Research Center program (2010-0001842) and the World Class University Program (R31-2008-000-10092) through the National Research Foundation of Korea (NRF) grant funded by the Ministry of Education, Science and Technology (MEST). Additionally, we appreciate the financial support of MKE (The Ministry of Knowledge Economy), Korea, under the ITRC (Information Technology Research Center) support program supervised by the NIPA (National IT industry Promotion Agency) (NIPA-2010-C1090-1021-0004).

## ■ REFERENCES

(1) O'Regan, B.; Gratzel, M. *Nature* **1991**, *353*, 737.
(2) Gratzel, M. *Inorg. Chem.* **2005**, *44*, 684.
(3) Xia, J.; Masaki, N.; Jiang, K.; Yanagida, S. *J. Mater. Chem.* **2007**, *17*, 2845.
(4) Li, Z.; Ye, B.; Hu, X.; Maa, X.; Zhang, X.; Deng, Y. *Electrochem. Commun.* **2009**, *11*, 1768.
(5) Li, Q.; Wu, J.; Tang, Q.; Lan, Z.; Li, P.; Lin, J.; Fan, L. *Electrochem. Commun.* **2008**, *10*, 1299.
(6) Ramasamy, E.; Lee, J. *Chem. Commun.* **2010**, *46*, 2136.
(7) Murakami, T. N.; Gratzel, M. *Inorg. Chim. Acta* **2008**, *361*, 572.
(8) Wang, G.; Xing, W.; Zhuo, S. *J. Power Sources* **2009**, *194*, 568.
(9) Ahmad, S.; Yum, J.-H; Xianxi, Z; Gratzel, M.; Butt, H.-J; Nazeeruddin, M. K. *J. Mater. Chem.* **2010**, *20*, 1654.
(10) Wang, Y. *J. Phys.: Conf. Ser.* **2009**, *152*, 012023.
(11) Saito, Y.; Kitamura, T; Wada, Y; Yanagida, S. *Chem. Lett.* **2002**, *31*, 1060.
(12) Saito, Y.; Kubo, W.; Kitamura, T.; Wada, Y.; Yanagida, S. *J. Photochem. Photobiol., A* **2004**, *164*, 153.
(13) Shibata, Y.; Kato, T.; Kado, T.; Shiratuchi, R.; Takashima, W.; Kaneto, K.; Hayase, S. *Chem. Commun.* **2003**, 2730.
(14) Kim, J. Y.; Jung, J. H.; Lee, D. E.; Joo, J. *Synth. Met.* **2002**, *126*, 311.
(15) Fan, B.; Mei, X.; Sun, K.; Ouyang, J. *Appl. Phys. Lett.* **2008**, *93*, 143103.
(16) Hong, W.; Xu, Y.; Lu, G.; Li, C.; Shi, G. *Electrochem. Commun.* **2008**, *10*, 1555.
(17) Wang, M.; Anghel, A. M.; Marsan, B.; Ha, N. L. C.; Pootrakulchote, N.; Zakeeruddin, S. M.; Gratzel, M.. *J. Am. Chem. Soc.* **2009**, *131*, 15976.
(18) Yoon, C. H.; Vittal, R.; Lee, J.; Chae, W. S.; Kim., K. J. *Electrochim. Acta* **2008**, *53*, 2890.
(19) Rowley, J. G.; Farnum, B. H.; Ardo, S.; Mayer, G. J. *J. Phys. Chem. C Lett.* **2010**, *1*, 3132.
(20) Bard, A. J.; Faulkner, L. R. *Electrochemical Methods: Fundamentals & Applications*; John Wiley & Sons: New York, 1980, p 218.
(21) Wang, M.; Anghel, A. M.; Marsan, B.; Ha, N.-L.; Pootrakulchote, N.; Zakeeruddin, S. M.; Gratzel, M. *J. Am. Chem. Soc.* **2009**, *131*, 15976.
(22) Tang, Y; Pan, X.; Zhang, C.; Dai, S.; Kong, F.; Hu, L.; Si, Y. *J. Phys. Chem. C* **2010**, *114*, 4160.